Low temperature laser absorption spectra of methane in the near-infrared at 1.65 μm for lower state energy determination*

Gao Wei(高 伟)[a)b)], Chen Wei-Dong(陈卫东)[c)], Zhang Wei-Jun(张为俊)[a)b)], Yuan Yi-Qian(袁怿谦)[a)b)], and Gao Xiao-Ming(高晓明)[a)b)†]

[a)] *Key Laboratory of Atmospheric Composition and Optical Radiation, Chinese Academy of Sciences, Hefei* 230031, *China*

[b)] *Anhui Institute of Optics and Fine Mechanics, Chinese Academy of Sciences, Hefei* 230031, *China*

[c)] *Laboratoire de Physicochimie de l'Atmosphère, Université du Littoral Côte d'Opale, 189A, Av. Maurice Schumann,* 59140 *Dunkerque, France*

(Received 11 July 2011; revised manuscript received 6 September 2011)

Direct absorption spectra of the $2\nu_3$ band of methane (CH_4) from 6038 to 6050 cm^{-1} were studied at different low temperatures using a newly developed cryogenic cell in combination with a distributed feedback (DFB) diode laser. The cryogenic cell can operate at any stabilized temperature ranging from room temperature down to 100 K with temperature fluctuation less than ±1 K within 1 hour. In the present work, the CH_4 spectra in the range of 6038–6050 cm^{-1} were recorded at 296, 266, 248, 223, 198, and 176 K. The lower state energy E'' and the rotational assignment of the angular momentum J were determined by a "2-low-temperature spectra method" using the spectra recorded at 198 and 176 K. The results were compared with the data from the GOSAT and the recently reported results from Campargue and co-workers using two spectra measured at room temperature and 81 K. We demonstrated that the use of a 2-low-temperature spectra method permits one to complete the E'' and J values missed in the previous studies.

Keywords: methane, laser absorption spectroscopy, cryogenic cell, low temperature absorption spectrum

PACS: 42.68.Ca, 25.20.Dc, 78.20.Ci **DOI:** 10.1088/1674-1056/21/1/014211

1. Introduction

Methane is the second most important greenhouse gas in the Earth's atmosphere, next to carbon dioxide. It plays a central role in atmospheric oxidation chemistry at regional and global levels and affects the concentrations of OH and O_3. It is one of the recommended key atmospheric gases[1] to be measured by GAW (global atmosphere watch) and EMEP (European Monitoring and Evaluation Program). In the solar system, methane exists almost everywhere. Infrared absorption of methane has a strong impact on the atmospheres of the Earth and the outer planets. Understanding CH_4 absorption spectra under different environmental conditions (temperature, pressure) could help us to sense and model the extraterrestrial atmospheres. For instance, the temperature of the Earth's atmosphere varies with latitude and the lowest temperature can be 180 K, while the temperature in the tropopause of Saturn's satellite Titan can be down to ∼ 71 K. The current spectroscopic knowledge of CH_4 spectra at low temperature is insufficient for the needs of state-of-the-art atmospheric modeling. In addition, the spectrum of methane is usually very congested at room temperature which has resulted in unsatisfactory spectral interpretation. The CH_4 line parameters (in particular at low temperature) included in the HITRAN 2008 databases,[2] such as rovibrational assignments of the angular momentum J and the lower state energy of the absorption transitions E'', are not well determined, particularly for wavelength shorter than 1.7 μm. Thus, recording and analysis of CH_4 spectra at low temperature are of considerable interest for atmospheric sciences and planetology. Methane at low temperature also allows us to reduce the congestion of absorption spectrum and simplify rovibrational analysis. Low temperature of CH_4 spectra can be obtained by direct sample cooling, by supersonic expansions, or by collisional cooling.[3−9]

*Project supported by the National Natural Science Foundation of China (Grant No. 41175036).

†Corresponding author. E-mail: xmgao@aiofm.ac.cn

© 2012 Chinese Physical Society and IOP Publishing Ltd

Spectra recorded at two different temperatures can be used for determination of the lower state energy level E'' by the ratio of the temperature-dependent line intensities.[4−13] Recently, Campargue and coworkers reported new progress in determination of the lower state energy of CH_4 transitions in the near infrared by using the so called "2-temperature spectra method". A temperature stabilized cryogenic cell was used to record CH_4 absorption spectra at a fixed cryogenic temperature.[14] The lower state energy values E'' and the angular momentum J values have been determined in the spectral region of 5852–6181 cm^{-1},[15,16] which is based on the ratio of the line intensities at room temperature (RT) and 81 K. In their reported work, the temperature of the cryogenic cell was not adjustable; it was kept at a fixed temperature, i.e., at 81 K. As the absorption features vary with temperature, some absorption lines disappear and some new ones appear, which might result in missing of the values of E'' and J for several lines when the room temperature spectra are compared with those at 81 K. Since at room temperature, line broadening and rotational congestion induced by the Doppler effect are more important than that at low temperature, line intensity determination may be more affected by blended lines which results in missing of spectral information for certain lines. It would be desirable to be able to work at any two cryogenic temperatures,[17] relatively close and stable enough for the determination of E'' and J using the 2-low-temperature spectra method, which makes absorption line identification easy and allows for accurate determination of absorption line intensity.

In the present work, we study the $2\nu_3$ band absorption spectrum of methane in the range of 6038–6050 cm^{-1} at low temperature with the help of a newly developed cryogenic cell. In the cryogenic cell, the flow of liquid nitrogen is controlled to achieve a desired temperature varying from room temperature to 100 K with high temperature stability ($\Delta T < \pm 1$ K). The methane absorption spectra were recorded at 296, 266, 248, 223, 198, and 176 K. The lower state energy E'' and rotational assignment of the angular momentum J were determined from the absorption spectra recorded at 198 and 176 K. We find that using the 2-low-temperature spectra method allows us to complete the E'' and J parameters missed for some absorption lines in the previously reported study[15] of using an RT spectrum associated with a low temperature spectrum at 81 K.

2. Spectroscopic consideration

In direct absorption spectroscopy,[18,19] the transmission of light radiation T_ν at a frequency of ν through a uniform medium of length L (in unit of cm) can be described by the Lambert-Beer law, which is given by

$$T_\nu = \frac{I_\mathrm{t}(\nu)}{I_0} = \exp\left[-k(\nu)L\right], \tag{1}$$

where $k(\nu)$ (in unit of cm^{-1}) is the spectral absorption coefficient, and $I_\mathrm{t}(\nu)/I_0$ is the ratio of the transmitted intensity to the incident intensity. The product $k(\nu)L$ is known as the spectral absorbance $\alpha_\nu(\nu)$

$$\alpha_\nu(\nu) = \ln\left(I_0/I_\mathrm{t}(\nu)\right) = k(\nu)L = N\sigma(\nu)L, \tag{2}$$

where N is the number of absorbing molecules per cubic centimeter (in unit of cm^{-3}), and $\sigma(\nu)$ is the frequency-dependent absorption cross section (in unit of cm^2). The integrated absorbance A_I (in unit of cm^{-1}) can be written as

$$\begin{aligned} A_\mathrm{I} &= \int \alpha_\nu(\nu)\mathrm{d}\nu = \int \ln\left(I_0/I(\nu)\right)\mathrm{d}\nu \\ &= NL\int \sigma(\nu)\mathrm{d}\nu = NLS, \end{aligned} \tag{3}$$

where $S = \int \sigma(\nu)\mathrm{d}\nu$ is the absorption line intensity (in unit of cm^{-1}).

The line intensity $S(T)$ can thus be determined by integrating the experimentally measured spectral absorbance as a function of temperature

$$S(T) = S(T_0)\frac{Q(T_0)}{Q(T)}\exp\left[-\frac{hcE''}{k}\left(\frac{1}{T}-\frac{1}{T_0}\right)\right], \tag{4}$$

where h (in unit of J·s) is Planck's constant, c (in unit of cm/s) is the speed of light in vacuum, k (in unit of J/K) is the Boltzmann constant, $Q(T)$ is the molecular partition function, T_0 (in unit of 296 K) is the reference temperature, and E'' (in unit of cm^{-1}) is the lower state energy of the corresponding transition.

Equation (4) can also be expressed for any two temperatures T_1 and T_2 as

$$S(T_2) = S(T_1)\frac{Q(T_1)}{Q(T_2)}\exp\left[-\frac{hcE''}{k}\left(\frac{1}{T_2}-\frac{1}{T_1}\right)\right]. \tag{5}$$

Because the vibrational energies are much higher than the considered thermal energies, the vibrational contribution to the partition functions $Q(T_1)$ and $Q(T_2)$ can be neglected. In addition, the stimulated emission term from the upper level of the transition is extremely weak and can be neglected. Only the contribution of the rotation to the partition function has to be considered.[14,20,21] Based on these hypotheses, the

ratio of the molecular partition functions at T_1 and T_2 can be expressed as follows:

$$\frac{Q(T_1)}{Q(T_2)} = \left(\frac{T_1}{T_2}\right)^{3/2}. \quad (6)$$

The lower state energy E'' of the considered transition can be then deduced from the variation of the line intensities at any two temperatures

$$E'' = -\ln\left(\frac{S(T_2)\,T_2^{3/2}}{S(T_1)T_1^{3/2}}\right)\Bigg/\left[\frac{hc}{k}\left(\frac{1}{T_2}-\frac{1}{T_1}\right)\right]\Bigg|_{T_1}^{T_2}. \quad (7)$$

3. Experimental details

The low temperature apparatus is schematically shown in Fig. 1. The cryogenic cell consists mainly of a cryostat and a sample cell, which is similar to the apparatus reported in Ref. [22]. The sample cell, 40 cm in length and $\phi = 2$ cm in diameter, is inside a vacuum chamber ($< 10^{-8}$ Torr), which can insulate the sample cell and the cryostat from any heat exchange with the external environment. The sample cell consists of a cold block (made of oxygen-free high-conductivity copper) and two aluminum tubes as cell arms terminated with CaF_2 windows wedged at a 3° angle to avoid unwanted interference fringes. An identical pair of CaF_2 windows, which are set unparallel to the former, are used as vacuum chamber windows. The cold block is attached to the cryostat. By controlling the liquid nitrogen flowing through the cold block of the cryostat, the temperature of the sample cell can be varied from room temperature to 100 K and stabilized at $\Delta T < \pm 1$ K within 1 hour. In the present work, a high precision flow valve is used to realize a cooling rate of about 1 K/min. The temperature of the cell is measured with three sensors (PT100, 70–1100 K) attached to the cell body: one sensor is located in the middle and the other two at the opposite ends of the sample cell. The precision of the temperature measurement is 0.5%. More details of our newly developed low temperature apparatus will be reported in Ref. [23].

The direct absorption spectra of CH_4 were recorded using the cryogenic cell described above. The arrangement of the experiment is schematically shown in Fig. 2. The spectral light source is a fiber-coupled single-mode InGaAsP distributed feedback (DFB) diode laser (NTT Electronics Corporation) operating at 1.65 μm and tunable from 6038 to 6050 cm^{-1} without mode hops. The laser output power is about 10 mW with a linewidth of ~ 2 MHz. The diode laser current and temperature are controlled by an LDC-3724B laser driver (ILX lightwave Inc.) with a short-term (1h) temperature stability < 0.004 °C and a long-term (24h) temperature stability < 0.01 °C. A function generator provides a scanning voltage to the laser driver for laser frequency varying from 6038 to 6050 cm^{-1} in conjunction with the laser temperature variation (from 10 °C to 40 °C). A 1×2 (1:99) fiber splitter is used to divide the laser beam into two parts. One part (1%) is connected to a wavelength meter (Wavemeter WA 1500) to measure the laser wavelength with a relative precision of ± 0.0002 cm^{-1}, and the main part (99%) is directed to the sample cell. An optical isolator (−30 dB) is used for each beam to minimize the optical feedback to the diode laser. The laser beam emerging from the absorption cell is focused onto an InGaAs photodiode. A multifunction DAQ card is used to digitize and record the spectral signal from the photodetector.

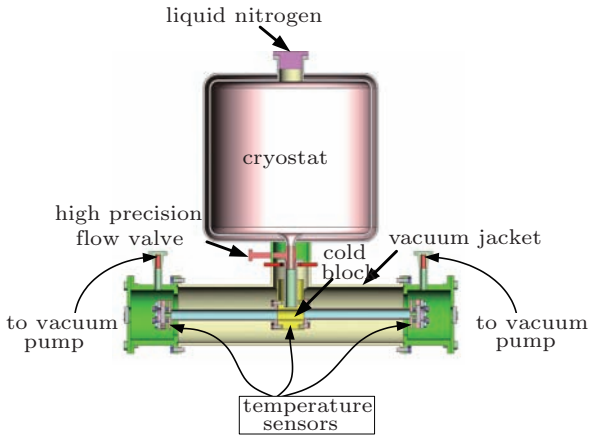


Fig. 1. (colour online) Schematic diagram of the newly developed low temperature apparatus. The cryogenic cell consists of a cryostat, a sample cell, three temperature sensors, a vacuum chamber, vacuum jacket, a high precision flow valve, and CaF_2 windows.

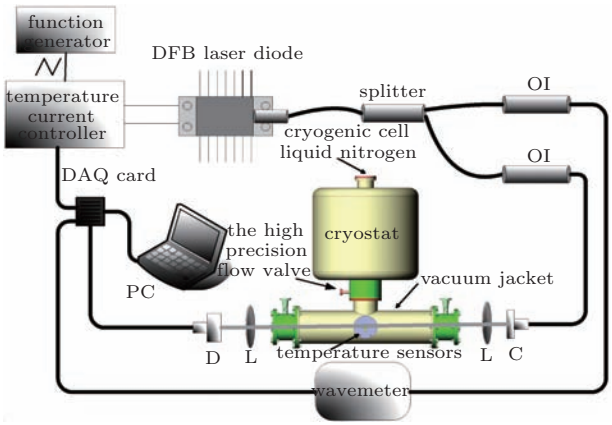


Fig. 2. (colour online) Schematic diagram of the experimental arrangement for low temperature CH_4 absorption spectroscopy. OI: optical isolator, L: lens, C: fiber coupler, D: detector.

4. CH_4 spectra in 6038–6050 cm^{-1} spectral region

Direct absorption spectra of 99.99% pure CH_4 were recorded at different temperatures ranging from RT to 176 K. The laser current was varied from 40 to 100 mA. For each spectral segment (~ 1 cm^{-1}), CH_4 spectra were acquired by averaging 1000 laser sweeps at a scanning rate of 30 Hz, and 1800 data points were acquired in each sweep. During the spectral acquisition, the CH_4 pressure was continuously measured with a capacitance gauge (MKS Baratron).

Spectral analysis for E'' and J determination consists of (i) spectrum baseline correction, (ii) absorption line identification, and (iii) integrated absorbance calculation. The Voigt profile is used to fit the experimental data with Gaussian width fixed to its theoretical value usually in the range of 215–280 MHz (HWHM). Compared with this Doppler induced linewidth, the DFB laser linewidth of about 2 MHz is neglected.

The laser baseline intensity I_0 is inferred by fitting part of the experimental spectra without absorption features with a third-order polynomial function. The representative data for the CH_4 transition at $\nu_0 = 6042.43$ cm^{-1} associated with a best-fit Voigt profile is shown in Fig. 3. The residual peak is less than 0.2%, which indicates that the Voigt profile adequately models the absorption line shape under the experimental conditions in the present work.

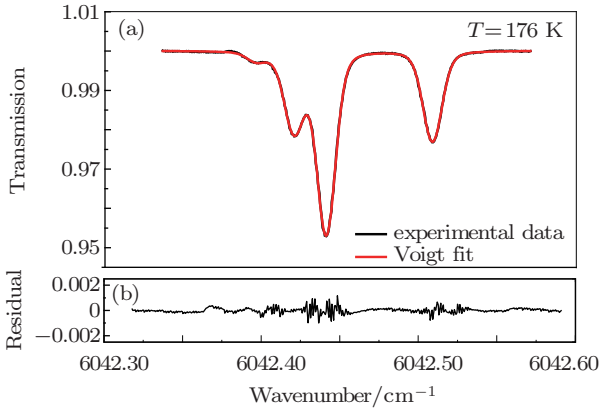


Fig. 3. (colour online) An example of CH_4 absorption spectrum recorded at 176 K. (a) The experimental spectrum (black line) at $P = 10.85$ Torr (1 Torr=133.3 Pa) and $L = 40$ cm, in comparison with the corresponding Voigt profile fit (red line); (b) the Voigt fit residual. The y axis is the integrated absorption $-\ln(I_t/I_0)/L$.

4.1. Characteristics of temperature-dependent CH_4 spectra

The CH_4 spectra of the $2\nu_3$ band recorded in the 6038–6050 cm^{-1}range are presented in Fig. 4. These were recorded at 296, 248, 223, 198, and 176 K with a pure CH_4 pressure of 26.4, 21.5, 16.9, 12.4, and 10.85 Torr, respectively. Figure 5 shows a portion of the spectra around 6039.7 cm^{-1}. Comparing the CH_4 spectra recorded at different temperatures in Figs. 4 and 5, we can clearly observe that some parts of the spectra are hardly recognizable at different temperatures. In addition, the absorption line broadening decreases when the temperature decreases, which can improve the spectral resolution and help determine spectral line intensity with high accuracy. It can be also observed in Figs. 4 and 5 that the temperature-dependent line intensity changes are considerable in some spectral regions. When the sample gas temperature is lowered by liquid nitrogen cooling, some line intensities decrease, some increase, and some new lines are observed. This is due to the fact that the absorption transitions from the lower J level increase when the temperature decreases, while the absorption transitions from the higher level J decrease, following the Boltzmann distribution rule.

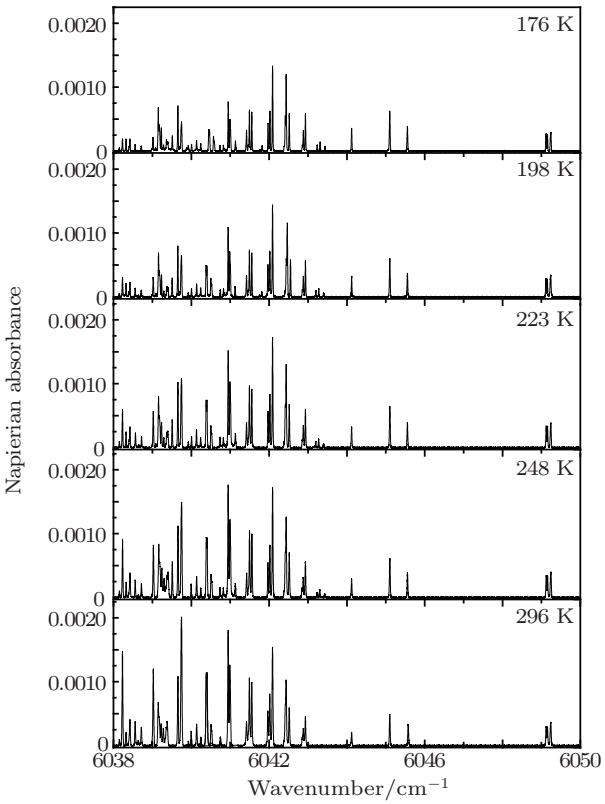


Fig. 4. Absorption spectra of CH_4 at 296, 248, 223, 198, and 176 K, with a pure CH_4 pressure of 26.4 , 21.5, 16.9, 12.4, and 10.85 Torr, respectively.

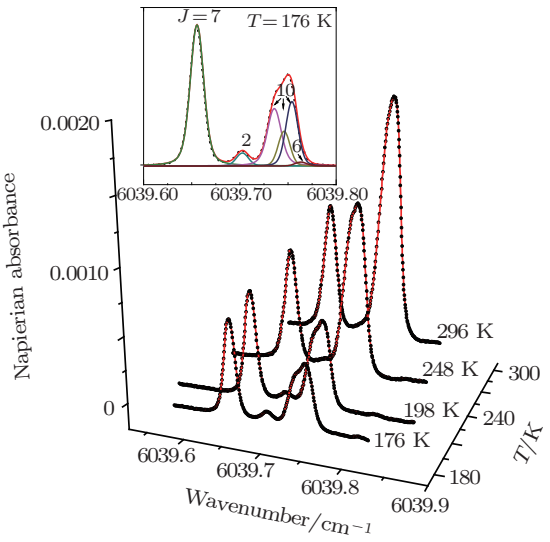


Fig. 5. (colour online) Temperature-dependent evolution of methane absorption spectra near 6039.75 cm^{-1}. The corresponding J values and the comparison between the experimental and fitted results are given in the insert.

4.2. Determination of E'' and J parameters

As long as line intensities are accurately measured, the lower state energy value E'' may be determined by the ratio of the line intensity values at two different temperatures by using Eq. (7). Then, the J value can be calculated by $E'' \approx B_0 J(J+1)$, where $B_0 = 5.214$ cm^{-1} in the present study. This method has been successfully applied to methane in a number of studies.[14–16,20] Here, the influence of centrifugal distortion is neglected because its value of $D_s = 1.085 \times 10^{-4}$ cm^{-1} is much smaller than B_0. The uncertainty in J value is mainly due to the uncertainty in E'' determination.

Based on Eq. (4), $\ln(S(T)T^{3/2}/(S(T_0)T_0^{3/2}))$ versus $1/T$ is expected to be linear with a slope equal to the lower state energy E'' of the considered transition. We experimentally checked this linearity by plotting the temperature-dependent line intensities of the lines at 6049.12 cm^{-1} ($J = 6.27$) and 6049.15 cm^{-1} ($J = 6.38$) versus $1/T$. The results are presented in Fig. 6. The linear dependence of $\ln(S(T)T^{3/2}/(S(T_0)T_0^{3/2}))$ on $1/T$ shows that the 2-temperature method is a valid empirical method and it can be used between "any two temperatures" for lower state energy determination. Based on this experimental demonstration, we decided to use the 2-low-temperature spectra for E''-value determination in the present work in order to complete the previous studies that used an RT spectrum associated with a low temperature spectrum for the 2-temperature spectra method.

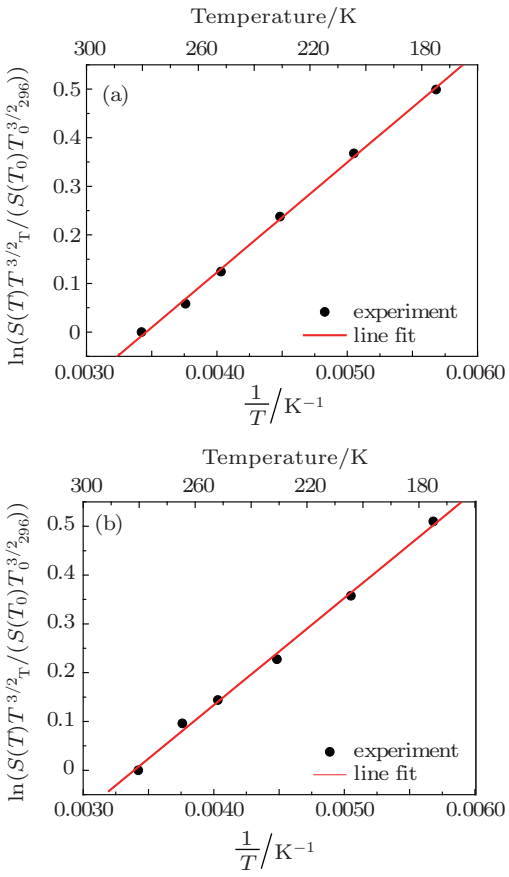


Fig. 6. Plot of $\ln(S(T)T^{3/2}/(S(T_0)T_0^{3/2}))$ versus $1/T$ at 296, 266, 248, 223, 198, and 176 K. The CH_4 lines at (a) 6049.12 cm^{-1} ($J = 6.27$) and (b) 6049.15 cm^{-1} ($J = 6.38$), respectively.

Two spectra acquired at 198 and 176 K respectively were used. The results are summarized in Table 1, including the line center positions, the line intensities, the lower state energy E'' and the J values. Parts of the data from GOSAT and from a recently published Ref. [15] are also given for comparison. The J assignments from GOSAT were determined either on the basis of a theoretical model or by applying the 2-temperature spectra method (between room temperature and low temperature) to FT–IR spectra of CH_4. The results from Ref. [15] were obtained by using laser absorption spectra recorded at RT and 81 K (the room temperature data at $T = 296$ K were from the GOSAT). GOSAT's J values and the results deduced from our 2-low-temperature spectra at 198 and 176 K agree well and the difference is $< \pm 1$, while the difference of some J values of Ref. [15] from our data is $> \pm 1$ and $< \pm 2$. For a number of lines, the disagreement can be explained by the blending of absorption lines at RT and very weak line intensities ($\sim 10^{-25}$ cm/molecule) at both RT and low temperature, which can lead to inaccurate determination of

line intensities. In certain cases, absorption line intensities at room temperature are much weaker than that at low temperature. For example, the absorption line at 6044.1225 cm^{-1} ($J = 2.08$) has a line intensity of 10^{-24} cm/molecule at room temperature, and it may increase to 10^{-23} cm/molecule at $T = 198$ K. Therefore, using the spectra recorded at two low temperatures could reduce uncertainty in line intensity ratio and thus improve the precision of the E'' and J values for these lines. In the present work, the typical noise equivalent absorption is 10^{-6} cm^{-1}, corresponding to a detection threshold on the order of 10^{-25} cm/molecule for line intensity. As can be observed in Table 1, for certain lines, the E'' and J values could not be determined in Ref. [15], which is probably due to the fact that the line intensities of some absorption lines cannot be determined, which results from the blending of lines in the congested RT spectrum.

Table 1. Line center position and line intensity of the methane transitions recorded from 6038 to 6050 cm^{-1} at 176 and 198 K, respectively. The determined lower state energy E'' and Jvalues are compared with the data from GOSAT and Ref. [15].

Line center/cm^{-1}	Line intensity/cm·molecular^{-1}		E''/cm^{-1}		J_{low}		
	$T = 176$ K	$T = 198$ K	This work	Ref. [15]	This work	GOSAT	Ref. [15]
6038.1502	1.21×10^{-24}	1.43×10^{-24}	376.054	390.263	8.00	8	8.14
6038.2310	7.47×10^{-24}	1.31×10^{-23}	812.960		11.99	12	
6038.3303	7.03×10^{-24}	7.31×10^{-24}	236.937	224.879	6.25	6	6.07
6038.4116	3.17×10^{-24}	3.22×10^{-24}	212.867	222.515	5.91	6	6.04
6038.4327	5.71×10^{-24}	6.76×10^{-24}	377.892	384.989	8.02	8	8.09
6038.5655	3.09×10^{-24}	4.51×10^{-24}	608.563	535.261	10.31	10	9.62
6038.7206	2.62×10^{-24}	3.68×10^{-24}	568.745	558.811	9.95	10	9.84
6038.9968	6.71×10^{-25}	6.90×10^{-25}	224.986	143.278	6.08	6	4.75
6039.0238	8.32×10^{-24}	1.31×10^{-23}	695.865	598.599	11.06	11	10.20
6039.0863	2.52×10^{-24}	2.83×10^{-24}	322.460	287.632	7.38	7	6.93
6039.1570	2.99×10^{-23}	2.82×10^{-23}	129.192	129.154	4.50	4	4.49
6039.1796	8.22×10^{-24}	7.64×10^{-24}	114.788	109.023	4.21	4	4.09
6039.1944	9.81×10^{-24}	9.21×10^{-24}	125.134	93.804	4.42	4	3.76
6039.2331	1.38×10^{-23}	1.28×10^{-23}	109.322	98.006	4.10	4	3.85
6039.2903	3.64×10^{-24}	4.70×10^{-24}	475.535	462.535	9.06	9	8.91
6039.3385	6.68×10^{-25}	8.88×10^{-25}	494.881		9.25	9	
6039.3634	5.51×10^{-24}	6.13×10^{-24}	312.132	302.467	7.25	7	7.11
6039.3873	4.75×10^{-24}	6.26×10^{-24}	497.316	465.145	9.27	9	8.93
6039.4012	1.77×10^{-24}	1.95×10^{-24}	301.153	321.470	7.11	7	7.35
6039.5096	7.64×10^{-24}	1.02×10^{-23}	509.807	469.677	9.40	9	8.98
6039.6579	2.55×10^{-23}	2.85×10^{-23}	316.542	301.591	7.30	7	7.10
6039.7057	1.79×10^{-24}	1.46×10^{-24}	33.513	65.676	2.08	2	3.08
6039.7397	1.25×10^{-23}	1.80×10^{-23}	596.953		10.21	10	
6039.7421	1.28×10^{-23}	1.82×10^{-23}	581.333	525.708	10.07	10	9.53
6039.7531	1.31×10^{-23}	1.85×10^{-23}	475.578		10.00	10	
6039.7583	3.41×10^{-24}	3.52×10^{-24}	229.193	230.797	6.14	5	6.16
6039.8770	1.89×10^{-24}	1.85×10^{-24}	166.317	161.172	5.17	5	5.07
6039.8949	1.76×10^{-24}	1.51×10^{-24}	25.162	23.652	1.75	1	1.68
6039.9252	2.55×10^{-24}	2.49×10^{-24}	176.825	198.850	5.34	6	5.68
6040.0041	3.57×10^{-24}	4.30×10^{-24}	398.370	394.072	8.25	8	8.19
6040.1426	6.11×10^{-24}	7.11×10^{-24}	362.268	384.876	7.85	8	8.08
6040.2100	3.34×10^{-25}	2.92×10^{-25}	45.106		2.48	2	
6040.2471	4.10×10^{-24}	4.25×10^{-24}	232.483	236.858	6.19	6	6.24
6040.3845	1.18×10^{-23}	1.53×10^{-23}	476.223	468.337	9.07	9	8.97
6040.4055	1.25×10^{-23}	1.59×10^{-23}	459.699	470.080	8.90	9	8.98

Table 1. (*Continued*).

Line center/cm^{-1}	Line intensity/cm·molecular^{-1}		E''/cm^{-1}		$J_{\rm low}$		
	$T = 176$ K	$T = 198$ K	This work	Ref. [15]	This work	GOSAT	Ref. [15]
6040.5051	8.98×10^{-24}	9.31×10^{-24}	233.966	228.182	6.21	6	6.12
6040.5260	6.51×10^{-24}	6.68×10^{-24}	223.365	228.162	6.06	6	6.12
6040.7424	3.08×10^{-24}	3.41×10^{-24}	305.803	304.372	7.17	7	7.14
6040.8260	2.65×10^{-24}	2.88×10^{-24}	286.493	308.434	6.92	7	7.19
6040.8557	2.99×10^{-24}	3.01×10^{-24}	201.612	156.328	5.73	5	4.98
6040.9479	2.89×10^{-23}	3.51×10^{-23}	410.058	385.142	8.38	8	8.09
6040.9895	1.65×10^{-23}	2.00×10^{-23}	408.107	329.259	8.36	8	7.44
6041.0064	1.05×10^{-23}	1.24×10^{-23}	375.463	382.788	8.00	8	8.06
6041.1265	7.78×10^{-24}	7.80×10^{-24}	196.392	157.506	5.65	5	5.01
6041.4089	1.81×10^{-24}	1.76×10^{-24}	161.121	111.732	5.08	5	4.14
6041.4241	1.19×10^{-23}	1.21×10^{-23}	212.609	167.347	5.90	5	5.17
6041.4685	2.10×10^{-24}	2.21×10^{-24}	250.424	224.827	6.44	6	6.07
6041.4964	2.16×10^{-23}	2.41×10^{-23}	314.713	301.234	7.28	7	7.10
6041.5188	8.05×10^{-25}	8.91×10^{-25}	305.307	173.993	7.16	7	5.28
6041.5577	1.96×10^{-23}	2.18×10^{-23}	311.262	301.327	7.24	7	7.10
6041.7575	9.94×10^{-25}	1.08×10^{-24}	285.529		6.91	7	
6041.8115	2.85×10^{-24}	2.62×10^{-24}	102.657	108.596	3.96	4	4.08
6041.9749	1.44×10^{-23}	1.51×10^{-23}	242.103	222.728	6.33	6	6.04
6042.0230	2.34×10^{-23}	2.46×10^{-23}	249.275	227.163	6.43	6	6.10
6042.0910	4.94×10^{-23}	5.03×10^{-23}	214.135	193.109	5.92	6	5.59
6042.3868	2.01×10^{-24}	1.79×10^{-24}	66.810	68.927	3.11	3	3.16
6042.4251	1.91×10^{-23}	1.95×10^{-23}	217.072		5.97	5	
6042.4391	3.85×10^{-23}	3.61×10^{-23}	120.451	104.458	4.33	4	3.99
6042.5171	1.99×10^{-23}	2.03×10^{-23}	216.165	159.219	5.95	5	5.03
6042.8552	2.53×10^{-24}	2.84×10^{-24}	321.384		7.36	7	
6042.8827	1.15×10^{-23}	1.06×10^{-23}	110.915	103.188	4.13	4	3.97
6042.9357	2.10×10^{-23}	1.87×10^{-23}	66.722	75.641	3.11	3	3.33
6043.2346	3.32×10^{-24}	2.88×10^{-24}	37.938	26.382	2.24	2	1.80
6043.3867	5.11×10^{-24}	4.53×10^{-24}	61.797		2.97	3	
6043.4389	2.61×10^{-24}	2.27×10^{-24}	40.802	30.126	2.34	2	1.95
6044.1225	1.25×10^{-23}	1.08×10^{-23}	33.530	2.160	2.08	2	0.31
6045.1054	3.53×10^{-23}	3.01×10^{-23}	19.042	25.042	1.47	1	1.74
6045.5603	1.94×10^{-23}	1.65×10^{-23}	16.814	29.135	1.36	1	1.91
6049.1227	1.23×10^{-23}	1.28×10^{-23}	238.097	159.010	6.27	6	5.03
6049.1581	1.09×10^{-23}	1.14×10^{-23}	245.779	159.733	6.38	6	5.04
6049.2301	8.54×10^{-24}	8.77×10^{-24}	223.505	151.419	6.06	6	4.90
6049.2441	1.34×10^{-23}	1.43×10^{-23}	264.061	166.561	6.63	6	5.16

In Fig. 7, we present a scatter graph of the determined lower state energy E'' values versus the transition line frequencies. The E'' values are indicated with their corresponding J values calculated from $E'' \approx B_0 J(J+1)$. From this graph, we can see how the experimentally determined J quantum numbers are close to integer values. In general, the empirical J values are quite close to integers. The determined J values far from integers are mainly due to the inaccurate line intensities.

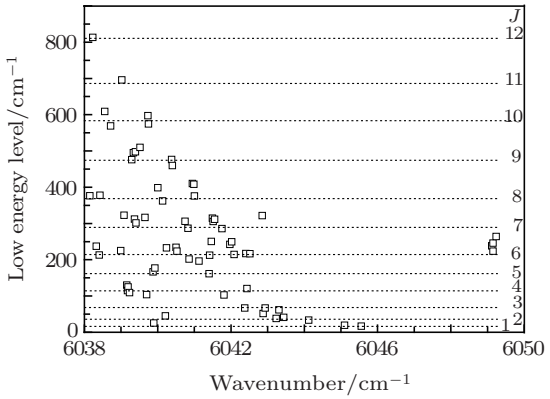


Fig. 7. A scatter graph of the lower state energy E'' values, obtained from the analysis of the methane spectra recorded at 176 and 198 K, versus the line centers for the region of 6038–6050 cm^{-1}. The values of the lower state energy rotational levels are indicated together with their corresponding J values.

5. Conclusion

Direct absorption laser spectra of the $2v_3$ band of methane were studied at low temperatures using a newly developed cryogenic cell. Spectra of CH_4 in the range of 6038–6050 cm^{-1} were recorded at different temperatures. The lower state energy E'' and rotational assignment of the angular momentum J were determined by using 2-low-temperature spectra recorded at 198 and 176 K.

We demonstrated that the use of 2-low-temperature spectra method for determining E'' and J permits one to complete the studies in which the E'' and J values of some absorption lines were missing because their line intensities were not determinable, which results from the seriously rotational congestion of the CH_4 spectrum at RT. This study can provide enhanced spectral information on methane line lists for atmospheric and planetary applications.

Acknowledgements

The support of the Groupement de Recherche International SAMIA between CNRS (France), RFBR (Russia) and CAS (China) is acknowledged.

References

[1] Müller G 2008 *A Contribution to the Implementation of the WMO Strategic Plan:* 2008–2011 (WMO TD NO. 1384) GAW report, No. 172. World Meteorological Organization, Geneva, Switzerland

[2] Rothman L S, Gordon I E, Barbe A, *et al.* 2009 *J. Quant. Spectrosc. Radiat. Transfer.* **110** 533

[3] Boras K, Deboer D, Lin Z and Reilly J P 1993 *J. Chem. Phys.* **99** 1429

[4] Campargue A, Chenevier M and Stoeckel F 1991 *Chem. Phys. Lett.* **183** 153

[5] Campargue A, Permogorov D and Jost R 1995 *J. Chem. Phys.* **102** 5910

[6] Hippler M and Quack M 1999 *Chem. Phys. Lett.* **314** 273

[7] Hippler M and Quack M 2002 *J. Chem. Phys.* **116** 6045

[8] Amrein A, Quack M and Schmitt U 1988 *J. Phys. Chem.* **92** 5455

[9] Albert S, Bauerecker S, Boudon V, Brown L R , Champion J P, Loëte M, Nikitin A and Quack M 2009 *Chem. Phys.* **356** 131

[10] Boraas K, Deboer D, Lin Z and Reilly J P 1994 *J. Chem. Phys.* **100** 7916

[11] Li H Y and Liu J S 2010 *Acta Phys. Sin.* **11** 7850 (in Chinese)

[12] Sun J M, Zhao G F, Wang X W, Yang W, Liu Y and Wang Y X 2010 *Acta Phys. Sin.* **11** 7830 (in Chinese)

[13] Margolis J S 1989 *Appl. Opt.* **27** 4038

[14] Kassi S, Gao B, Romanini D and Campargue A 2008 *Phys. Chem. Chem. Phys.* **10** 4410

[15] Gao B, Kassi S and Campargue A 2009 *J. Mol. Spectrosc.* **253** 55

[16] Wang L, Kassi S and Campargue A 2010 *J. Quant. Spectrosc. Radiat. Transfer.* **111** 1130

[17] Votava O, Mašát M, Pracna P, Kassi S and Campargue A 2010 *Phys. Chem. Chem. Phys.* **12** 3145

[18] Baer D S, Nagali V, Furlong E R, Hanson R K and Newfield M E 1996 *AIAA J.* **34** 489

[19] Nagali V, Chou S I, Baer D S, Hanson R K and Segall J 1996 *Appl. Opt.* **35** 4026

[20] Margolis J S 1990 *Appl. Opt.* **27** 2295

[21] Fox K 1970 *J. Quant. Spectrosc. Radiat. Transfer.* **10** 1335

[22] Lewis E K, Moehnke C J, Navea J G and Manzanares C E 2006 *Rev. Sci. Intrum.* **77** 073107

[23] Gao W, Chen W D, Zhang W J, Yuan Y Q and Gao X M *Spectroscopy and Spectral Analysis* (accepted)